Investigation of the use of radiomics for analysis of DAT-SPECT imaging in Parkinson's disease

Silvia Moro
University of Padova
2089329

Emma Roveroni
University of Padova
2058618

Abstract

***Background**: We aim to investigate the use of radiomics features for analysis of DAT-SPECT imaging in Parkinson's disease in order to understand their utility as a biomarker of this pathology.* ***Methods**: We consider 53 cases of both healthy control (HC, n=20) and PD (n=33) groups, from the Pet Node Repository available at the King's College London and 11 classes of 177 radiomics features applied to DAT SPECT imaging in putamen ROI. Firstly, Least Absolute Shrinkage and Selection Operator (LASSO) is used to reduce redundancy of the dataset. A first statistical analysis with Mann Whitney U and Kruskal-Wallis tests is carried out to verify differences in radiomics features between the two groups. Spearman correlation is performed to explore the association between PD symptoms severity, based on clinical tests, and radiomics features. Finally five different machine learning models (i.e. logistic regression, k-NN, decision tree, random forest and SVM) are used to investigate classification performance through their accuracy and their ROC AUC score.* ***Results:** For the majority of the features, their values are found to be significantly different between patients and controls. Some significant correlations (p-values$<$0.05) with clinical tests are observed especially for UPDRS III test, but they are not so strong. Finally, radiomics features appear to be extremely good predictors for classifying HC and PD: all the accuracies achieved are higher than 85%, same goes for ROC AUC metric ($>$90%). Despite these exciting results, we need to consider the small dimension of our dataset, which can lead the model to be less prone to generalization.* ***Conclusions**: Radiomics features applied to DAT SPECT imaging differ between patients with Parkinson and healthy subjects and they have potentials in classifying the two groups, so they may be useful as an aid to the diagnosis of PD. The same cannot be said about their correlation with Parkinson's clinical symptoms severity, which results are quite poor.*

1. Background

Parkinson's disease (PD) is one of the most common progressive neurodegenerative movement disorders, with an incidence rate estimated between 8 and 18 per 100 000 person-years [1]. Pathologically, PD is characterized by the degeneration of dopaminergic nigro-striatal neurons and by accumulation of misfolded α-synuclein, founded in intracytoplasmic inclusions called Lewy bodies [1] [2].
Dopamine is a neurotransmitter synthesized in the pars compacta of substantia nigra and carried along a bundle of fibers to the striatum in the basal ganglia, which comprises the caudate nucleus and putamen [3]. The degeneration of the nigrostriatal pathway leads to a wide range of motor symptoms, such as tremors, bradykinesia, rigidity, and postural abnormalities, as well as non-motor symptoms, such as dementia, psychiatric symptoms like depression and anxiety, sleep disturbance, gastrointestinal disorders, cardiovascular problems [1] [2].
Although PD is a clinical diagnosis, imaging is now part of the routine examination. Dopamine transporter (DAT) single-photon emission computed tomography (SPECT) provides a SPECT image showing the loss in the striatum of DAT binding, which is the protein that normally regulates dopamine transport and dopamine reuptake in presynaptic cells [4] [5]. This technique furnishes an objective measure of the dopaminergic nerve cell loss in vivo, and contributes to management of patients who do not fully meet the diagnostic criteria of PD or show mild symptoms in the early stage, also avoiding misdiagnosis, such as essential tremor (ET), Alzheimer's disease and vascular pseudoparkinsonism [4] [5]. The most commonly used and commercially available radiotracers for this analysis are 123I-FP CIT and 123I-beta-CIT, which have shown high sensitivity for detecting a binding reduction in PD compared with healthy controls (HC) [4] [5].
Generally, the evaluation of DAT-SPECT images is conducted via visual inspection, frequently supported by a semi-quantitative analysis, which is effective in eliminating subjectivity and experience differences. Despite this, they

do not represent the homogeneity or heterogeneity of radiopharmaceutical distribution in the striatum [6].
The introduction of radiomics, following the increase in the digitization of information and the development of artificial intelligence (AI), represented a more objective assessment in the analysis of images, giving information imperceptible to the human eye [7]. It is an image analysis technique, based on the extraction of quantitative metrics both from 2-dimensional (2D) regions of interest (ROIs) or 3-dimensional (3D) volumes of interest (VOIs). They are called radiomics features and can be divided into many classes, related to the intensity of the pixels/voxels of the image and geometrical properties: histogram-based; texture-based; model-based; transform-based; and shape-based [8][9].
In recent years, radiomics is expected to be used for diagnosis as well as for predicting patient prognosis and for determining treatment effects, with a wide application in oncology [9].
It has recently been extended to other medical applications such as neurodegenerative diseases and there is emerging literature about this topic. Kang JJ et al. [10] confirmed its crucial role in diagnosing PD and assessing cognitive impairment (CI), while Shiiba et al. [6] constructed a radiomics signature with the same aim. Moreover, Rahmim et al. [11] used Haralick texture measures, which have found increasing utility in the field of radiomics and heterogeneity quantification, highlighting correlations with severity of motor and cognitive symptoms in Parkinson's disease , while in Rahmim et al. [12] is demonstrated that radiomics features applied to DAT SPECT images have a significant potential towards development of effective prognostic biomarkers in PD.
The purpose of this report is to investigate the impact of radiomics analysis for DAT SPECT imaging as a biomarker of Parkinson's Disease with 123I-FP CIT radiotracer, by analyzing the differences in the features between patients and controls and the association of them with PD clinical symptoms severity. Finally, we want to assess if radiomics features can effectively discriminate PD from HC and consequently evaluate their classification performance.

2. Materials and methods

2.1. Participants

The dataset used in this study is derived from the PET NODE REPOSITORY available at King's College London, and it refers to a set of radiomics features derived for DAT-SPECT imaging scans. The study involves 53 subjects, including n=33 idiopathic PD patients and n=20 healthy controls (HD). All the participants have received a screening visit, a clinical visit and also imaging assessment. Male and women selected were required to be age 30-85 years, agreed to ensure that they will use contraceptive measures to avoid respectively to impregnate the partner and to get pregnant for the duration of the study and for 3 months following the last administration of SPECT ligands. All male subjects must also agree to refrain from donating sperm during this time and postmenopausal females must have follicle-stimulating hormone (FSH) =38 mlU/mL at screen. Included PD subjects were diagnosed after the age of 30 years, classified in Hoehn and Yahr scale (H&Y) between stages 1 to 3, and they must never have been treated with levodopa or dopamine agonists, or are undergoing dopamine replacement therapy. From both groups were excluded participants who were taking serotonin acting drugs within 60 days prior to baseline and SPECT scans, who have other neurological disorders or recent history of drug/alcohol abuse. Furthermore, participants who had renal disease, clinical infection, significant blood clotting disorder or history of cancer within the last 5 years were left out from the study. Finally, patients with PD were excluded if they have received previous surgery, or have been treated with duodopa (or apomorphine), or had changed the pharmacologic therapy for PD's symptoms within 30 days prior to screen.
All patients underwent a screening, where their demographics were collected (age, gender, education, height, weight, BMI) and a clinical visit, where their neurological situation can be evaluated using the following clinical tests: (i) Unified Parkinson's Disease Rating Scale (UPDRS- parts I, II, III, IV), (ii) Non-Motor-Symptoms Questionnaire (NMSQ), (iii) Mini-Mental State Examination (MMSE), (iv) Montreal Cognitive Assessment (MoCA) score. It's also reported the value of (v) Levodopa Equivalent Daily Dose (LEDD) for each patient.
SPECT imaging scan was performed in all eligible participants 4+- 0.5h following injection of approximately 185 MBq of [123I]-FP-CIT, targeting the dopamine transporter system.

2.2. SPECT image pre-processing and calculation of Standard Uptake Value Ratios (SUVR)

For all the subjects, the imaging data analysis pipeline included the segmentation of brain anatomical regions using the CIC v2.0 neuroanatomical atlas and coregistration to the subject's structural MRI.
SPECT [123I]FP-CIT image volumes are spatially normalized to an [123I]FP-CIT template. The eight most prominent axial slices containing the striatum are summed and a standardized volume of interest (VOI) template is applied to this image. VOI analysis will be performed on putamen, used as the main region, employing the cerebellum region as the reference tissue.
Standardise Uptake Value Ratios (SUVRs), considered the main parameters of interest to represent presynaptic dopaminergic integrity and function, are calculated as the

ratio of the putamen VOI count density, divided by the cerebellum count density. This measure approximates the binding potential when the radioligand is in equilibrium at the target site and has previously been reported with [123I]FP-CIT SPECT.

2.3. Radiomics features extraction

Features were extracted for each subject using the MIRP Python package.
Calculations were performed in 3D: the ROI corresponding to the putamen was resegmented from the SUVR images to eliminate voxels with an intensity value below a threshold equal to 1.2 (selected after visual inspection of the available data). Discretisation was then performed by setting a fixed bin size of 0.0125 for the intensity histogram of the image. This value was set to have around 64 grey levels in the image. When necessary, features were aggregated using the 3D average method.
In the end, a total of 177 features were extracted for putamen VOI.

2.4. Radiomics features selection

Before starting the analysis, it was checked that the dataset did not contain any missing value and it has been fixed by removing features with the same value for each subject. All of the radiomics features were z-scored to mean 0 and standard deviation 1.0 and the least absolute shrinkage and selection operator (LASSO) function in Python (Version 3.10.11) was used to select effective features, in order to reduce the high redundancy between them [6][10][13]. LASSO permits the estimation and selection of explanatory variables, that is, radiomics features with nonzero coefficients.
All the following analyses were performed by taking into consideration only the features selected.

2.5. Statistical analysis

All the statistical analyses were performed using Python (Version 3.10.11).
For all the tests implemented in the work a statistically significant difference with p-value$<$0.05 was considered.
To make sure we were dealing with two homogeneous groups of PD e HC, we compared their demographics data with Mann Whitney U test and Fisher test for Gender [10][13].
Furthermore, demographics were studied more deeply to verify their correlation with the radomics features, in order to assess if there was the need to consider them in the successive analysis, in case they added more information.
After that, the focus was on the differences between PD and HC, in terms of radiomics features. A first analysis was made by observing the distributions of the values in the two groups; then two statistical non-parametric tests were performed: Mann Whitney U and Kruskal-Wallis.
Statistical analysis then continued by calculating comparable correlation [10][13] between radiomics features and the results of the specific clinical tests § 2.1, in order to determine a possible association with the severity of Parkinsonian symptoms.
Further confirmation was given through the Kruskal-Wallis statistic test, considering the clinical test which presented more correlation with radiomics features and dividing the patients' data in low/moderate/high severity, following the literature.

2.6. Classification models construction using machine learning

All models were constructed using Python (Version 3.10.11).
First of all, radiomics features were z-scored to mean 0 and standard deviation 1.0. Then, the patients in the dataset were randomly divided into training set and test set, with a ratio of 7:3. Five classification models for the HC and PD groups were constructed: logistic regression, k-nearest neighbor (KNN), random forest, decision tree and support vector machine (SVM) [14].
In order to establish which values for the hyperparameters of these models were the best ones, a grid search on the training set was performed for each model.
The main parameters for each of the classier were the following: for Logistic regression (fit_intercept = True, max_iter = 10000, penalty = None); for k-NN (n_neighbors = 3); for decision tree (criterion = gini, max_depth = None, min_sample_split = 2); for random forest (criterion = gini; max_depth = None; n_estimator = 5); for SVM (C=0.1, kernel = linear).
After that, to better train the model, a 10-fold cross-validation was implemented using the training set.
Classification performances were evaluated using accuracy and area under the ROC curve (AUC).

3. Results

The first thing that we observe is the absence of missing values in the dataset and the presence of a feature with all the same values for each patient, which can be removed because it is useless.

3.1. LASSO features selection

As mentioned before, LASSO method was adopted in order to perform feature selection, with the main parameter alpha = 0.008986, selected as optimal with an automatic cross-validation.
The total number of features selected by LASSO is 19 and they can be seen in Table 1; the selection includes at the same time histogram, shape and texture features.

Table 1: **Radiomics features selected using LASSO**

Feature family	Selected Features
Intensity-based statistics	stat_qcod
Intensity-volume histogram	ivh_v50
	ivh_diff_v25_v75
	ivh_diff_i25_i75
Intensity histogram	ih_min_fbs_w0.0125
	ih_iqr_fbs_w0.0125
	ih_max_grad_g_fbs_w0.0125
Morphology	morph_comp_2
	morph_com
	morph_pca_maj_axis
	morph_pca_elongation
	morph_area_dens_aee
	morph_area_dens_conv_hull
	morph_moran_i
GLCM	cm_clust_shade_d1_3d_avg_fbs_w0.0125
	cm_info_corr2_d1_3d_avg_fbs_w0.0125
GLSZM	szm_lzlge_3d_fbs_w0.0125
GLDZM	dzm_sdlge_3d_fbs_w0.0125
NGLDM	ngl_hdlge_d1_a0.0_3d_fbs_w0.0125

GLCM grey level co-occurrence matrix; *GLSZM* grey level size zone matrix; *GLDZM* grey level distance zone matrix; *NGLDM* neighbouring grey level dependence matrix

3.2. Demographics statistics

In Table 2 are shown the characteristics of the demographics data.

Table 2: **Participants demographics**

Feature	PD	HC
Number of subjects	33	20
Age	60.54 ± 9.52	63.10 ± 8.58
Male/female	21/12	15/5
Education (Years)	15.78 ± 3.58	16.55 ± 3.44
Height	169.98 ± 10.07	173.52 ± 8.56
Weight	78.06 ± 16.32	81.43 ± 12.04
BMI	26.98 ± 4.98	27.11 ± 4.14

As it's possible to see, the difference between PD and HC in terms of age, education, height, weight, BMI and sex, is not huge. This can be observed both by just focusing on their mean value.
By visual inspection, as we can see in Figure 1, it is assessed that demographics are not normal; for this reason, for the comparison we considered the non-parametric Mann Whitney U test for covariates "Age", "Education", "Height", "Weight" and "BMI", while for categorical "Gender" variable we adopted the Fisher test.

Even the results given by the test, presented through

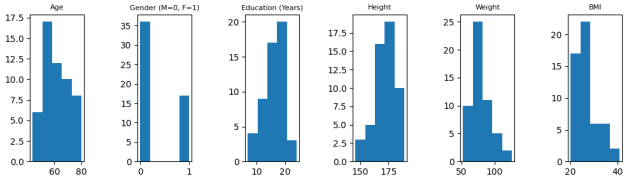

Figure 1: **Demographics distribution**

Table 3: **Demographics data statistic tests results**

Feature	p-value
Age	0.37
Male/female	0.54
Education (Years)	0.62
Height	0.18
Weight	0.28
BMI	0.61

the p-values in Table 3 (all $p > 0.05$), confirm that the two groups don't show significant differences, thus it is reasonable to assume that they are homogeneous and comparable. To further investigate the demographics data and their relationship with radiomics features, Spearman correlations were computed between the two set of variables.
What emerges from the results of the correlation analysis is that there is not enough correlation to consider the covariates in our subsequent analysis.

3.3. Analysis of difference between PD and HC in radiomics features

First of all we notice, as it is possible to see in Figure 2, that there is no evidence of normal distribution in the selected features. After dividing the dataset between PD e HC, Figure 3 shows in a first analysis the distribution of each radiomics features in the two groups, highlighting the differences. Subsequently, the two tests mentioned in § 2.5 were implemented and in Table 4 we summarize the results. Both have identified the same 14 features out of the initial 19 as significantly different.

3.4. Radiomics features' association with PD clinical symptoms severity

Significant results of Spearman correlation between clinical tests and selected radiomics features are reported in Table 5 and shown in Figure 4. Despite the features and the clinical measures don't manifest such a strong correlation, as we can see in the value of correlation coefficients, we place our attention in the relationships that showed a p-value statistically significant ($p<0.05$). It can be noticed that in some clinical tests, there isn't evidence of correlation with the radiomics features: they are UPDRS I, UPDRS IV and

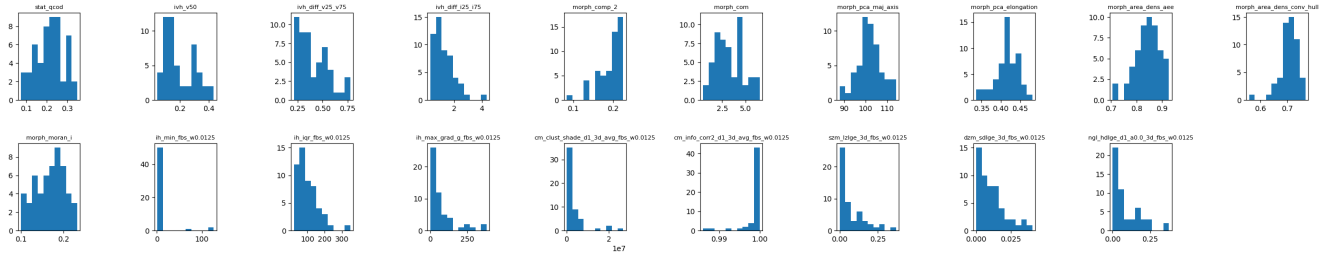

Figure 2: **Distribution of radiomics features**

also the measure of LEDD. All the others show significant results at least with one of the features, while UPDRS III is found to be the only one to have a greater number of correlations, in particular with morphological features.
To support our findings, we also divided the radiomics features into groups based on the classification of their disease severity: this division depends on cut-offs found by Martínez-Martín at al. [15] e resumed in Table 6. With the Kruskal-Wallis test we compare every division of the features and of the UPDRS in order to see if there is an association. We added this method just to confirm our results and also in this case UPDRS III is the test with the most links, with the same features as before plus others.

Table 4: **Results of statistic tests for radiomics distribution comparison between PD and HC**

Feature	Mann Whitney U p-value	Kruskal-Wallis p-value
stat_qcod	1.67e-08	1.58e-08
ivh_v50	3.64e-09	3.45e-09
ivh_diff_v25_v75	2.56e-08	2.42e-08
ivh_diff_i25_i75	1.27e-08	1.21e-08
morph_comp_2	2.90e-04	2.79e-04
morph_com	5.63e-05	5.41e-05
morph_pca_maj_axis	3.35e-01	3.30e-01
morph_pca_elongation	1.65e-01	1.63e-01
morph_area_dens_aee	5.75e-02	5.63e-02
morph_area_dens_conv_hull	8.47e-01	8.40e-01
morph_moran_i	1.35e-02	1.32e-02
ih_min_fbs_w0.0125	5.15e-01	5.04e-01
ih_iqr_fbs_w0.0125	1.27e-08	1.21e-08
ih_max_grad_g_fbs_w0.0125	1.38e-02	1.35e-02
cm_clust_shade_d1_3d_avg_fbs_w0.0125	4.64e-02	4.54e-02
cm_info_corr2_d1_3d_avg_fbs_w0.0125	3.21e-07	3.06e-07
szm_lzlge_3d_fbs_w0.0125	3.29e-06	3.15e-06
dzm_sdlge_3d_fbs_w0.0125	1.01e-05	9.76e-06
ngl_hdlge_d1_a0.0_3d_fbs_w0.0125	3.60e-06	6.40e-09

In blue are highlighted the statistically significant p-values.

Table 5: **Correlation between clinical data and radiomics features**

Clinical test	Correlated features	Correlation coeff.	p-value
UPDRS I	-	-	-
UPDRS II	morph_comp_2	-0.34	0.048
	morph_area_dens_conv_hull	-0.39	0.02
UPDRS III	stat_qcod	-0.43	0.01
	morph_comp_2	-0.36	0.03
	morph_pca_elongation	-0.41	0.01
	morph_area_dens_conv_hull	-0.53	0.001
	cm_clust_shade_d1_3d_avg_fbs_w0.0125	-0.34	0.04
UPDRS IV	-	-	-
UPDRS total	morph_comp_2	-0.41	0.017
	morph_area_dens_conv_hull	-0.47	0.005
NMSQ	ivh_v50	0.34	0.047
MMSE	stat_qcod	-0.36	0.039
MoCA	morph_area_dens_aee	0.35	0.04

UPDRS Unified Parkinson's Disease Rating Scale; *NMSQ* Non-Motor Symptoms Questionnaire; *MMSE* Mini-Mental State Examination; *MoCA* Montreal Cognitive Assessment.

Table 6: **Level of severity based on UPDRS test**

Clinical test	Mild/moderate	Moderate/severe
UPDRS I	10/11	21/22
UPDRS II	12/13	29/30
UPDRS III	32/33	58/59
UPDRS IV	4/5	12/13

UPDRS Unified Parkinson's Disease Rating Scale

3.5. Radiomics features for classification task

All the models we have tried to accomplish the prediction task have given similar results, both in terms of accuracy and ROC AUC curve.
The accuracies achieved with the models, which can be seen in Figure 5, are quite high. In particular, the Random forest seems to be the one which is most precise in distinguishing between PD and HC, reaching an accuracy value of 93%. All the other models behaved almost as well, with an ac-

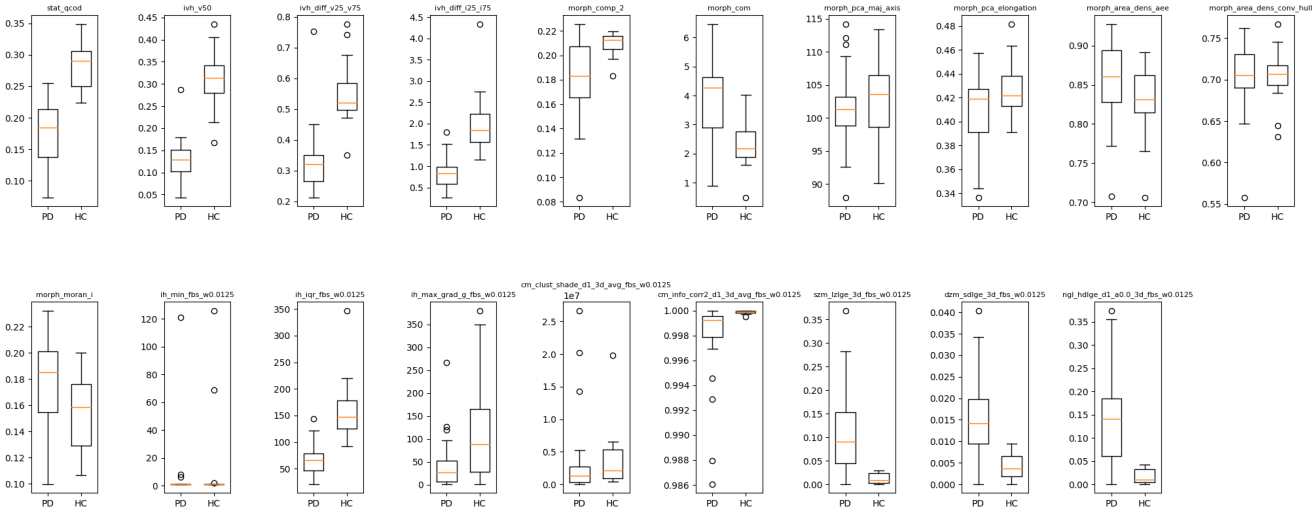

Figure 3: **Difference in distribution of radiomics features between PD and HC**

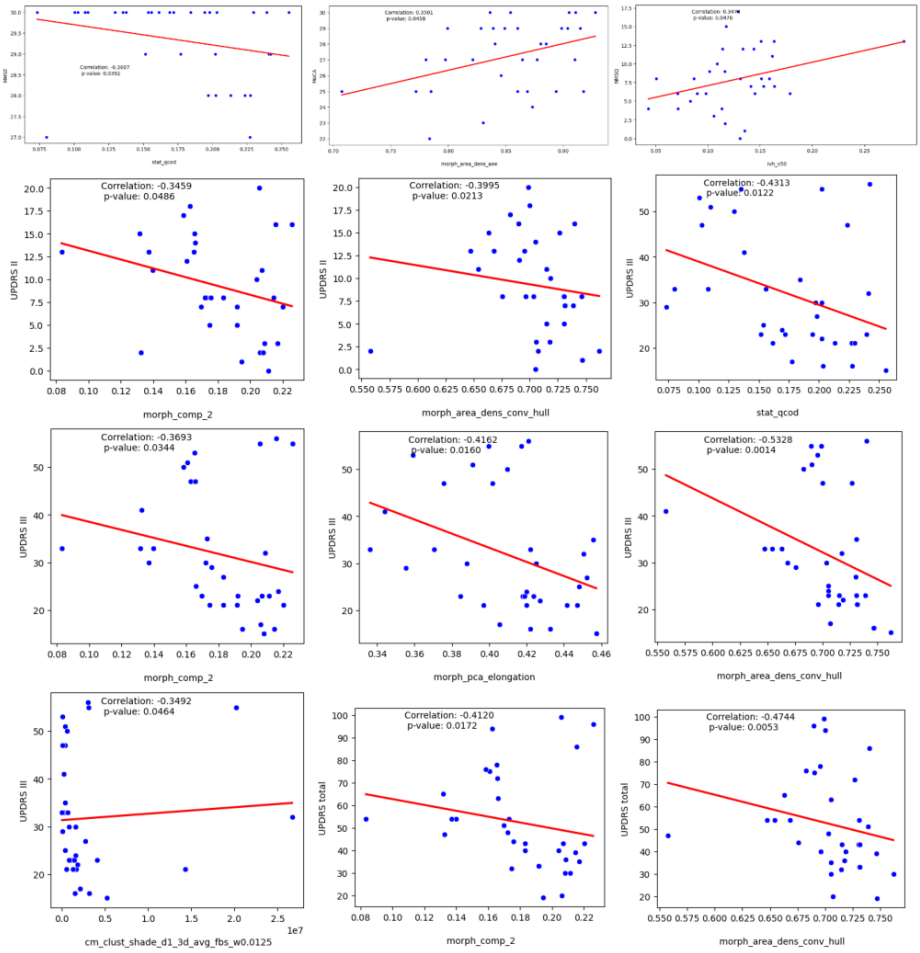

Figure 4: **Correlation between radiomics features and clinal tests**

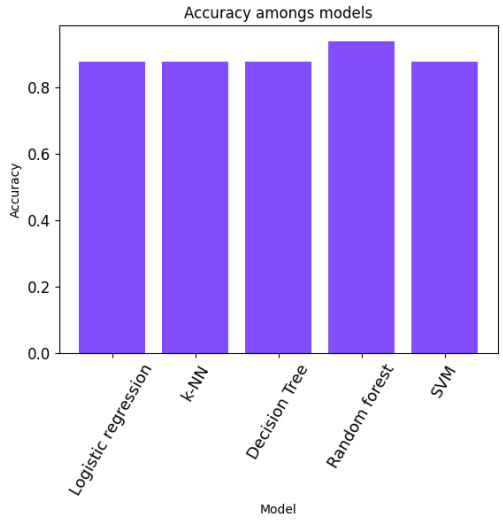

Figure 5: **Models' accuracy in prediction task**

curacy of 87%. Even the score obtained by the ROC AUC curve are very high and similar among the models, as it is possible to observe in Figure 6. To further support these results, in Figure 7 we reported the confusion matrices given by each model. As we can observe, the models have learned how to classify the two groups quite well.

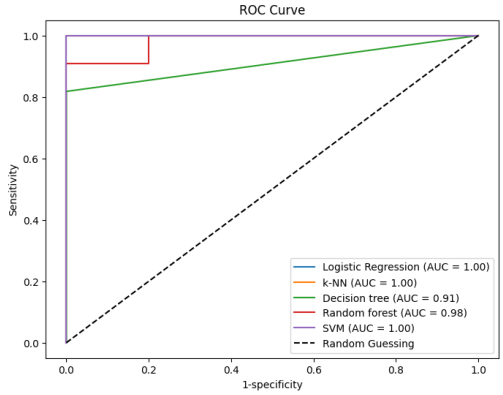

Figure 6: **Comparison of models' ROC AUC**

4. Discussion

In this study we investigate the use of radiomics for analysis of DAT-SPECT imaging in Parkinson's disease, in order to understand their power as a biomarker for this neurological disorder.

Both by visual inspection and by statistical tests the difference in the values of the radiomics features between PD and HC is found to be significant by the majority, confirming

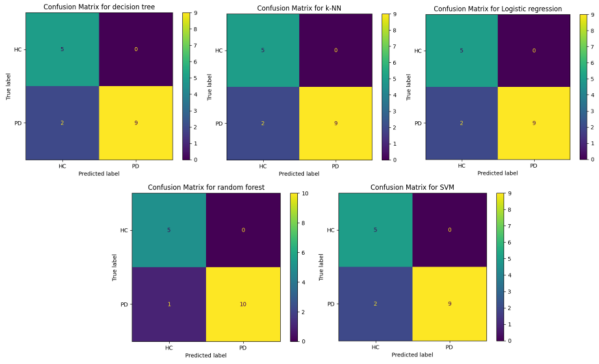

Figure 7: **Confusion matrices for each model**

what we could see in Shiiba T et al. [6] with the comparison of the radiomic signature of the two groups, which was constructed as a linear combination of the most important features.

Talking about association with PD clinical symptoms severity, we don't find many significant correlations between radiomic features and clinical tests. The most correlated results to be UPDRS III test. UPDRS is the most widely used scale to measure impairment and disability in PD and the third part refers to the clinician motor examination [16]: as we know, the motor symptoms are the most common and evident in parkinsonian patients. UPDRS III is also the most widely considered part of the UPDRS test in the literature when dealing with the correlation between clinical features and symptoms. i.e. Rahmim A. et al. [11], Rahmim A et al. [12]. With the correlation, the family of morphological features, also called shape-based, turns out to be the most significant. The importance of the shape in PD patients is due to the fact that DAT-SPECT images in normal controls have a comma shaped structure, which is lost in PD patients because of the decreasing striatal radiotracer uptake. In particular, since putamen is more severely affected in early-stage PD and it has greater loss of DAT binding, the striatum appears with an oval or circular appearance on SPECT images [4], [5], [17].

For what regards the ability of radiomics features to distinguish between PD and HC, interesting results were achieved. In particular all the machine learning models that we have developed have accomplished very high performances. These results are exciting, but we need to be aware that they also may be a little bit deceptive. In fact in this study we are involving a dataset of small size. This may influence the models' performances since the model is trained on a few samples, possibly making the model less prone to generalize.

Another common pitfall that frequently affects radiomics studies is the class imbalances [9]. As we can see our dataset is quite unbalanced and for this reason the model

can struggle more when it has to learn and then predict the minority class. This may suggest that our models are good for the prediction task, and so that radiomics features are actually quite helpful when we want to distinguish between PD and HC, but to further verify this it would be interesting to test the models on more and unseen data.
Another compelling fact is related to the confusion matrices given by the machine learning models. In particular we are referring to the fact that most of the models seems to predict incorrectly some PD patients, classifying them as HC. This is a situation that we would like to avoid because the model is missing patients affected by Parkinson, having as consequences a missing diagnosis and so a delayed treatment.
In the future it is necessary to consider increasing the number of cases, in order to have more reliable results. Moreover, a multimodal approach that analyzes the combination of the application of radiomics features to more imaging techniques (SPECT as in our analysis, PET [18], MRI [19]) can improve the robustness of the study.

5. Conclusions

The role of radiomics features applied to DAT SPECT images as a biomarker of Parkinson's Disease is still unclear and complex. Certainly their values differ between patients with Parkinson and healthy subjects, but the poor correlation with routine clinical trials does not allow us to reach positive conclusions about their association with PD clinical symptoms severity. On the other hand, the performance of various classification models is very good, leading us to say that radiomics features derived images can help in distinguishing between PD and HC, although our analysis has some limitations to consider.

References

[1] Roberta Balestrino and Anthony HV Schapira. Parkinson disease. *European Journal of Neurology*, 27(1):27–42, 2020. PMID: 31631455.

[2] Lorraine V Kalia and Anthony E Lang. Parkinson's disease. *Lancet*, 386(9996):896–912, 2015. PMID: 25904081.

[3] Marjorie Oliveira Klein, Daniele Schneiders Battagello, Alessandra Rodrigues Cardoso, Danielle Nascimento Hauser, Jackson Cioni Bittencourt, and Raul Gustavo Correa. Dopamine: Functions, signaling, and association with neurological diseases. *Cell Mol Neurobiol*, 39(1):31–59, 2019. PMID: 30446950.

[4] Thomas Brücke and Christoph Brücke. Dopamine transporter (DAT) imaging in Parkinson's disease and related disorders. *J Neural Transm (Vienna)*, 129(5-6):581–594, 2022. PMID: 34910248.

[5] Ülkü Özcan Akdemir, Ali Bora Tokçaer, and Levent Özdemir Atay. Dopamine transporter SPECT imaging in Parkinson's disease and parkinsonian disorders. *Turk J Med Sci*, 51(2):400–410, Apr 2021.

[6] Takeshi Shiiba, Keisuke Takano, Akihiro Takaki, and Shugo Suwazono. Dopamine transporter single-photon emission computed tomography-derived radiomics signature for detecting parkinson's disease. *EJNMMI Res*, 12(1):39, 2022. PMID: 35759054; PMCID: PMC9237203.

[7] Janna E Van Timmeren, Davide Cester, Stephanie Tanadini-Lang, Hatem Alkadhi, and Bettina Baessler. Radiomics in medical imaging-"how-to" guide and critical reflection. *Insights Imaging*, 11(1):91, 2020. PMID: 32785796.

[8] Stephen S Yip and Hugo JWL Aerts. Applications and limitations of radiomics. *Phys Med Biol*, 61(13):R150–R166, 2016. PMID: 27269645.

[9] Marius E Mayerhoefer, Andrzej Materka, Georg Langs, Ida Häggström, Piotr Szczypiński, Peter Gibbs, and Gary Cook. Introduction to radiomics. *J Nucl Med*, 61(4):488–495, 2020. PMID: 32060219.

[10] Jia-Jia Kang, Ying Chen, Gui-Dong Xu, Shi-Lin Bao, Jing Wang, Meng Ge, Li-Hua Shen, and Zhi-Zheng Jia. Combining quantitative susceptibility mapping to radiomics in diagnosing Parkinson's disease and assessing cognitive impairment. *Eur Radiol*, 32(10):6992–7003, Oct 2022.

[11] Arman Rahmim, Yousef Salimpour, Sanjay Jain, Steven A Blinder, Igor S Klyuzhin, Gwenn S Smith, Zoltan Mari, and Vesna Sossi. Application of texture analysis to DAT SPECT imaging: Relationship to clinical assessments. *Neuroimage Clin*, 12:e1–e9, 2016. PMID: 27995072.

[12] Arman Rahmim, Paul Huang, Nikolay Shenkov, Shahram Fotouhi, Esmaeil Davoodi-Bojd, Lijun Lu, Zoltan Mari, Hamid Soltanian-Zadeh, and Vesna Sossi. Improved prediction of outcome in Parkinson's disease using radiomics

analysis of longitudinal DAT SPECT images. *Neuroimage Clin*, 16:539–544, Aug 2017.

[13] Qiushi Ren, Ying Wang, Siwei Leng, Xiaopeng Nan, Bin Zhang, Xin Shuai, Jia Zhang, Xudong Xia, Yaqi Li, Yaxin Ge, Xiangyu Meng, and Cheng Zhao. Substantia nigra radiomics feature extraction of Parkinson's disease based on magnitude images of susceptibility-weighted imaging. *Front Neurosci*, 15:646617, May 2021.

[14] David Forsyth. *Applied Machine Learning*. Springer International Publishing, 2019.

[15] P. Martínez-Martín, C. Rodríguez-Blázquez, M. Alvarez, T. Arakaki, V. C. Arillo, P. Chaná, W. Fernández, N. Garretto, J. C. Martínez-Castrillo, M. Rodríguez-Violante, M. Serrano-Dueñas, D. Ballesteros, J. M. Rojo-Abuin, K. R. Chaudhuri, and M. Merello. Parkinson's disease severity levels and MDS-unified Parkinson's disease rating scale. *Parkinsonism Relat Disord*, 21(1):50–54, 2015.

[16] Christopher G Goetz, Barbara C Tilley, Stephanie R Shaftman, Glenn T Stebbins, Stanley Fahn, and et al. Martinez-Martin P. Movement disorders society sponsored revision of the unified Parkinson's disease rating scale: scale presentation and clinimetric testing results. *Movement Disorders*, 23:2129–2170, 2008.

[17] T. Shiiba, Y. Arimura, M. Nagano, T. Takahashi, and A. Takaki. Improvement of classification performance of Parkinson's disease using shape features for machine learning on dopamine transporter single photon emission computed tomography. *PLoS One*, 15(1):e0228289, 2020.

[18] Yan Wu, Jie-Hui Jiang, Lei Chen, Jing-Yuan Lu, Jing-Jing Ge, Feng-Tao Liu, Jin-Tai Yu, Wei Lin, Cheng-Tao Zuo, and Jin Wang. Use of radiomic features and support vector machine to distinguish Parkinson's disease cases from normal controls. *Annals of Translational Medicine*, 7(23):773, 2019.

[19] P. Liu, H. Wang, S. Zheng, F. Zhang, and X. Zhang. Parkinson's disease diagnosis using neostriatum radiomic features based on T2-weighted magnetic resonance imaging. *Frontiers in Neurology*, 11:248, 2020.